

PNAS

www.pnas.org

1

2 **Main Manuscript for**3 Hydrogen sulfide is neuroprotective in Alzheimer's disease by
4 sulfhydrating GSK3 β and inhibiting Tau hyperphosphorylation.5 Daniel Giovinazzo¹, Biljana Bursac⁵, Juan I Sbodio¹, Sumedha Nalluru¹, Thibaut Vignane⁵, Adele
6 M. Snowman¹, Lauren M. Albacarys¹, Thomas W. Sedlak², Roberta Torregrossa⁴, Matthew
7 Whiteman⁴, Milos R. Filipovic⁵, Solomon H. Snyder^{1,2,3*} and Bindu D. Paul^{1*}8 ¹The Solomon H. Snyder Department of Neuroscience, ² Department of Psychiatry and Behavioral
9 Sciences, ³Department of Pharmacology and Molecular Sciences, Johns Hopkins University
10 School of Medicine, Baltimore, MD 21205, United States. ⁴Medical School Building, University of
11 Exeter, Exeter, United Kingdom. ⁵Leibniz-Institut für Analytische Wissenschaften - ISAS - e.V.,
12 Dortmund, Germany.

13 Correspondence to:

14 * Bindu D. Paul; Solomon H. Snyder

15 **Email:** bpaul8@jhmi.edu16 ssnyder@jhmi.edu17 **Classification:** Biology, Neuroscience18 **Keywords**19 Alzheimer's disease, Hydrogen sulfide, Tau, Sulfhydration, Persulfidation, Cystathionine γ -lyase,
20 NaGYY21 **Author Contributions**22 BDP conceptualized the study. BDP, DG and SHS designed the study. DG, BDP, BB, JIS, SN, TV,
23 AMS and MRF conducted experiments. MW and RT provided synthesized ultra-pure H₂S donors
24 and helped design animal dosage. TWS provided tools/reagents. LMA helped with animal care,
25 genotyping and maintenance. DG, MRF, SHS and BDP analyzed data. DG, SHS and BDP wrote
26 the paper with input from all the authors.27 **This PDF file includes:**

28 Main Text, Figures 1 to 4

29

30 **Abstract**

31

32 Alzheimer's disease (AD), the most common cause of dementia and neurodegeneration in the
33 elderly, is characterized by deterioration of memory, executive and motor functions.
34 Neuropathologic hallmarks of AD include neurofibrillary tangles, paired helical filaments and
35 amyloid plaques. Mutations in the microtubule associated protein, Tau, a major component of the
36 neurofibrillary tangles, cause its hyperphosphorylation in AD. We have shown that signaling by the
37 gaseous signaling molecule, hydrogen sulfide (H₂S), is dysregulated during aging. H₂S signals via
38 a posttranslational modification termed sulfhydration/persulfidation, which participates in diverse
39 cellular processes. Here we show that cystathionine γ -lyase (CSE), the biosynthetic enzyme for
40 H₂S, binds wild type Tau, which enhances its catalytic activity. By contrast, CSE fails to bind Tau
41 P301L, a mutant that is hyperphosphorylated in the 3xTg-AD mouse model of AD. We further show
42 that CSE is depleted in 3xTg-AD mice as well as in human AD brains, H₂S prevents phosphorylation
43 of Tau by sulfhydrating its kinase, glycogen synthase kinase 3 β (GSK3 β). Finally, we demonstrate
44 that sulfhydration is diminished in AD, while administering the H₂S donor, sodium GYY4137
45 (NaGYY), to the 3xTg-AD mice ameliorates motor and cognitive deficits in AD.

46 **Significance Statement**

47 Alzheimer's disease (AD) is the leading cause of dementia in the elderly. Although dysregulated
48 hydrogen sulfide (H₂S) metabolism has been reported in AD, and H₂S donors are beneficial,
49 molecular mechanisms underlying neuroprotective effects of H₂S are largely unknown. We now
50 show that H₂S confers neuroprotection by sulfhydrating GSK3 β , to inhibit its activity, thereby
51 preventing hyper-phosphorylation of Tau, a key pathogenic event in AD. Administering H₂S donors
52 improves motor and cognitive functions in a mouse model of AD.

53

54 **Introduction**

55

56 Alzheimer's disease (AD), the most prevalent neurodegenerative disorder, involves loss of memory
57 and executive functions (1, 2). Currently no cure exists for AD, and clinical trials of diverse agents
58 have largely failed to demonstrate therapeutic benefit (3, 4). AD may occur sporadically or have a
59 genetic origin, with several mutations linked to a high risk for the disease (5). AD is characterized
60 by aggregation of the microtubule associated protein, Tau and β -amyloid peptides, which are
61 components of neurofibrillary tangles (NFTs) and amyloid plaques respectively (2, 3, 6). AD
62 belongs to the class of diseases termed tauopathies, which include progressive supranuclear palsy
63 (PSP), corticobasal degeneration (CBD), Pick's disease and frontotemporal lobar degenerative

64 disorders (FTLD) (7, 8). Tau was originally identified as a microtubule binding protein, which
65 mediates assembly of microtubules (9). Tau undergoes several post-translational modifications *in*
66 *vivo*, including phosphorylation, sumoylation and acetylation (10-13). Disease progression in AD is
67 closely linked to Tau pathology (14, 15). Hyperphosphorylation of Tau, a hallmark of AD, decreases
68 its binding to microtubules and causes its aggregation and mislocalization leading to neurotoxicity
69 via multiple mechanisms, including changes in cytoskeletal architecture, axonal transport and
70 mitochondrial respiration. (16-20).

71 AD is associated with increased oxidative stress which promotes neurodegeneration (21). The
72 reverse transsulfuration pathway leading to the synthesis of cysteine and glutathione (GSH) helps
73 maintain redox homeostasis in the brain (Fig. 1A) and is dysregulated in neurotoxicity and
74 neurodegeneration (22-26). Cystathionine γ -lyase (CSE) is the biosynthetic enzyme for the
75 gaseous signaling molecule hydrogen sulfide (H_2S) as well as its precursor cysteine (27)(Fig. 1A).
76 CSE utilizes cystathionine which is synthesized from homocysteine by cystathionine β -synthase
77 (CBS), to generate cysteine (28). Both CSE and CBS synthesize H_2S in the brain, with CSE
78 expressed in neurons and CBS in astrocytes (29). H_2S is formed endogenously in almost all tissues
79 and signals by sulfhydration/persulfidation (27, 30-33). Like nitric oxide (NO) and carbon monoxide
80 (CO), H_2S is a gasotransmitter with pleiotropic roles (27, 34). Apart from its role as an endothelial
81 derived relaxation factor (EDRF), H_2S has neuroprotective functions at physiological concentrations
82 (34-37). We have shown previously that disrupted metabolism of cysteine and H_2S may be
83 pathogenic in neurodegenerative conditions such as Parkinson's disease (PD) and Huntington's
84 disease (HD) (24, 25, 38). Sulfhydration is an evolutionarily conserved process, which is
85 diminished during aging (39). Depletion of cysteine, a product of the reverse transsulfuration
86 pathway, is also associated with aging and neurodegeneration (40, 41). We now report that the
87 reverse transsulfuration pathway and persulfidation are dysregulated in AD while supplementation
88 with H_2S donors is beneficial. Moreover, motor and cognitive deficits are mitigated by administration
89 of H_2S donors.

90 **Results**

91 **Dysregulation of the reverse transsulfuration pathway in AD**

92 Previously we reported altered H_2S metabolism and sulfhydration patterns in PD, while
93 administering H_2S donors proved beneficial in mouse models of PD (9, 10). Similarly, in mouse
94 models of AD, H_2S donors reversed disease symptoms and improved spatial and cognitive deficits
95 (42, 43). We analyzed the expression of CSE in AD mouse models as well as human post-mortem
96 samples. We utilized the 3xTg-AD mouse model of AD, which harbors the mutations PS1M146V,
97 APPSwe and Tau P301L and develops both neurofibrillary tangles and amyloid plaques (44). CSE
98 expression was reduced in the cerebral cortex and hippocampus of these mice (Fig. 1B,C).

99 Moreover, we observed a 50% decrease in CSE expression in the cortex of AD postmortem brain
100 (Fig. 1D). Using the dimedone-switch assay, we observed decreased levels of overall sulfhydrylation
101 (Fig. 1E,F).

102 **CSE and CBS interact with wild type but not Tau P301L**

103 As H₂S levels and sulfhydrylation are decreased in AD patients, we explored the interaction of CSE
104 and CBS, the major H₂S producing enzymes, with Tau and amyloid precursor protein (APP),
105 proteins, which constitute the NFTs and amyloid plaques respectively. Neither CSE nor CBS bound
106 APP (*SI Appendix*, Fig. S1A, B). In the adult brain Tau exists as six isoforms derived by alternative
107 splicing (45). We utilized full length Tau comprising 441 amino acid residues, which is also present
108 in neurons (46)(Fig. 2A). CSE and CBS bind to wild type Tau in HEK293 cells overexpressing CSE
109 or CBS and Tau (Fig. 2B). Next, we studied the interaction of Tau and CSE, purified from bacterial
110 cells (*SI Appendix*, Fig. S2). Purified CSE and Tau also interacted, indicating that CSE binds Tau
111 directly (Fig. 2C). As the 3xTg-AD mouse model harbors the mutant, Tau P301L, we studied the
112 binding of CSE and CBS to this mutant in HEK293 cells. Both CSE and CBS did not bind the P301L
113 mutant of Tau (Fig. 2D). In the case of CBS, using GFP-Tau, we observed additional bands
114 migrating above the band corresponding to GFP-Tau, likely reflecting non-specific bands (Fig. 2D).
115 In the case of Flag-Tau, additional bands were not observed (Fig. 2B). As Tau is a neuronal protein
116 and CSE, but not CBS, resides in neurons, with CBS being localized to astrocytes, we focused the
117 remainder of our studies on CSE. We analyzed the influence of Tau on CSE activity by measuring
118 H₂S production from L-cysteine in the presence of its cofactor, pyridoxal 5-phosphate (PLP).
119 Purified tau enhanced H₂S production from human recombinant CSE *in vitro* (Fig. 2E,F). We also
120 measured H₂S production (by supplementing with L-cysteine and PLP) from the lysates of HEK293
121 cells transfected with CSE and Tau (Fig. 2G). CSE activity increased with time, and wild type Tau
122 further augmented H₂S generation by CSE (Fig. 2H). As CSE is the biosynthetic enzyme for H₂S
123 in neurons and signals by sulfhydrylation, we assessed whether Tau is sulfhydrated by CSE. Tau
124 contains two cysteine residues, Cys291 and Cys322, which could be sulfhydrated (Fig. 2A). We
125 monitored Tau sulfhydrylation in transfected HEK293 cells using the modified biotin switch assay
126 (Fig. 2I), as well as the dimedone switch method in conjunction with mass spectrometry, which
127 revealed that Tau is indeed sulfhydrated at C322 (*SI Appendix*, Fig. S5).

128 **H₂S generated by CSE inhibits phosphorylation of Tau by glycogen synthase kinase β**

129 Tau harbors several sites which are phosphorylated by multiple kinases. Hyperphosphorylation of
130 Tau decreases its affinity for microtubules and causes its aggregation. One of the major kinases
131 which phosphorylates Tau is glycogen synthase kinase β (GSK3β), a serine/threonine kinase,
132 which modifies several sites on the protein *in vivo* (47). We wondered whether CSE and H₂S

133 modulate Tau phosphorylation by GSK3 β . To explore the effect of H₂S on Tau phosphorylation,
134 we utilized purified Tau, CSE and GSK3 β in an *in vitro* assay (Fig. 3A). Phosphorylation of Tau at
135 Ser396 by GSK3 β was significantly diminished when CSE in combination with L-cysteine and PLP,
136 the substrate and cofactor for CSE respectively, were added to the reaction mixture (containing
137 CSE, Tau and ATP as described in the Materials and Methods), indicating a role for H₂S. Consistent
138 with this observation, phosphorylation of Tau was reduced when sodium hydrosulfide (NaSH) was
139 added alone to GSK3 β , Tau and ATP, in the absence of CSE, L-cysteine and PLP (Fig. 3A). To
140 determine whether the cysteines in Tau affect its phosphorylation, we mutated these residues to
141 serine and conducted the phosphorylation assays with GSK3 β . Phosphorylation of the mutant, Tau
142 C291S/C322S, was inhibited as well, indicating that absence of cysteine residues does not prevent
143 the inhibition of Tau phosphorylation by GSK3 β (Fig. 3B). As GSK3 β is inhibited by phosphorylation
144 of its Ser9 residue by the endogenous kinase, Akt, we explored whether the inhibitory effect of H₂S
145 on phosphorylation of Tau involves Ser9 of GSK3 β . We utilized a constitutively active mutant of
146 GSK3 β , GSK3 β S9A, wherein Ser9 is mutated to Ala (and therefore is not subject to inhibition by
147 Akt) and examined the effect of H₂S on phosphorylation of Tau. We analyzed Tau phosphorylation
148 in HEK293 cells using the mutant, Tau P301L, which is a mutation present in the 3xTg-AD mouse
149 model of AD (44). NaSH inhibited phosphorylation of Tau P301L even when GSK3 β S9A was
150 present, indicating that H₂S acts by a mechanism independent of phosphorylation of GSK3 β at
151 Ser9 (Fig. 3C). Similarly, H₂S also inhibited phosphorylation of the C291S/C322S mutant of Tau
152 P301L in HEK293 cells, further confirming that inhibition of Tau phosphorylation does not require
153 the cysteine residues on Tau (Fig. 3C). In HEK293 cells, phosphorylation of Tau resulted in its
154 slower migration on gels, as reported previously (48). Treatment with NaSH inhibited
155 phosphorylation at Ser396 and resulted in faster mobility of Tau P301L on the gel (Fig. 3C). NaSH
156 also inhibited phosphorylation of Tau at Ser202 and Thr205 (*SI Appendix*, Fig. S3A). Moreover,
157 total Tau levels were increased in the GSK3 β transfected samples, which may reflect stabilization
158 of Tau P301L by GSK3 β , which could result in increased accumulation of Tau and neurotoxicity.
159 To further characterize inhibition of GSK3 β activity by H₂S, we conducted activity assays using
160 radioactive [γ -³²P]-ATP, GSK3 β and a peptide substrate of GSK3 β , monitoring phosphorylation of
161 the peptide by scintillation counting. Like the assays conducted earlier, NaSH significantly inhibited
162 phosphorylation of the peptide (*SI Appendix*, Fig. S3B). As HEK293 cells harbor other kinases such
163 as extracellular signal-related kinase-1 and -2, and mitogen-activated protein kinases, p38 kinase
164 and c-jun N-terminal kinase, which can also phosphorylate Tau, it remains to be determined
165 whether H₂S inhibits phosphorylation of Tau by these kinases (48). Thus, it appeared likely that
166 H₂S prevents phosphorylation of Tau by inhibiting GSK3 β , possibly by sulfhydrating it. Therefore
167 we examined the sulfhydration of GSK3 β using mass spectrometry, revealing that GSK3 β was
168 indeed modified by H₂S at Cys218 (*SI Appendix*, Fig. S4). A closer analysis of the sequence of

169 GSK3 β revealed that Cys218 lies close to Tyr216 which is phosphorylated in the kinase domain.
170 Moreover, 3D-modeling showed that Cys218 lies close to Asp181 in the active site, which is
171 involved in hydrogen bond formation for catalysis. Persulfidation or sulfhydration of Cys218 could
172 disrupt the active site conformation (Fig. 3D,E). We analyzed sulfhydration of GSK3 β in human AD
173 samples using the dimedone switch assay in combination with an antibody array method we
174 previously developed (39). In this method, a GSK3 β antibody is immobilized on a 96 well plate with
175 an *N*-hydroxysuccinimide (NHS)-activated surface as described previously (Fig. 3F) (39).
176 Considering that proteins are labelled with 4-chloro-7-nitrobenzofurazan (NBF, green) reflecting
177 total load and with cyanine-5 (Cy5, red) for sulfhydration, the ratio of these two signals would yield
178 the observed levels of GSK3 β sulfhydration. As a negative control 488-labelled albumin (instead of
179 antibody) was used to block the available surface and then incubated with control lysates. The
180 assay revealed that sulfhydration of GSK3 β was significantly diminished in the cortex of AD
181 patients, as compared to normal subjects (Fig. 3G,H). Sulfhydration of GSK3 β was decreased
182 almost two-fold in the cerebral cortex of AD patients, further confirming our observation that
183 sulfhydration is decreased in AD.

184 **H₂S donors alleviate behavioral symptoms in the 3xTg-AD mouse model**

185 To examine the neuroprotective effects of H₂S *in vivo*, we administered NaGYY, a synthetic sodium
186 salt derivative of Lawesson's reagent, N-benzoylthiobenzamide, GYY4137 and a slow releasing
187 H₂S donor to 3xTg-AD mice (49-52). Commercially available GYY4137 is synthesized as a
188 morpholine salt (morpholine is toxic and biologically active) and also contains undisclosed amounts
189 of the carcinogenic solvent (dichloromethane) which is metabolized to CO, potentially complicating
190 the interpretation of effects obtained. Accordingly, we utilized in-house ultrapure NaGYY (See
191 Materials and Methods for additional details), which is devoid of these confounding effects and has
192 been well characterized with the additional advantage of being water soluble (52, 53).

193 Mice were treated either with NaGYY or saline (vehicle) at 6-mo via daily intraperitoneal injections
194 (100 mg/kg in saline) for 12 wk. Levels of sulfhydration and behavioral studies were conducted 3-
195 mo after treatment with NaGYY at 9-mo. Overall levels of sulfhydration were decreased in the 3xTg-
196 AD mice, which was rescued in the 3xTg-AD mice treated with NaGYY (Fig. 4A). In addition, we
197 observed that sulfhydration of immunoprecipitated Tau is decreased in AD mice and restored in
198 NaGYY treated animals (Fig. 4B). Next, we studied the effects of the H₂S donor on motor and
199 cognitive functions of AD mice. We used an open field test to study the overall locomotor activity of
200 3xTg-AD mice treated with the H₂S donor. The AD mice had a reduced locomotor activity as
201 compared to the wild type mice. NaGYY treatment enhanced overall locomotor activity of the AD
202 mice (Fig. 4C). The most studied features of AD are memory impairments and cognitive deficits,

203 although non-cognitive deficits, such as motor dysfunction, are also present and may even precede
204 classical clinical symptoms (54). Motor symptoms have been observed in patients with autosomal
205 dominant AD which correlate with disease progression (55). Treatment with NaGYY partially
206 rescued memory deficits of 3xTg-AD mice in the Barnes maze memory tests at 9-mo as compared
207 to their vehicle (saline)-treated controls. The primary latency in the Barnes maze test was
208 significantly improved, but there was no significant change in the primary, total error, or total latency
209 in these mice (Fig. 4D-G). Thus, the H₂S donor NaGYY elicits beneficial effects on motor and
210 cognitive deficits of AD mice.

211

212 **Discussion**

213

214 The principal finding of this study is that the gasotransmitter, H₂S is neuroprotective in AD, by
215 inhibiting phosphorylation of Tau via sulfhydration of GSK3 β , the kinase for Tau. In addition, by
216 sulfhydrating cysteine residues on target proteins, H₂S prevents irreversible oxidation of cysteine
217 residues as demonstrated previously (39). Earlier we reported decreased H₂S signaling by
218 sulfhydration in PD, HD and during aging (24, 25, 39). Neuronal H₂S produced by CSE mediates
219 stress responses, which are compromised in neurodegenerative diseases (38, 56).

220 H₂S levels are tightly regulated in cells. Excess H₂S deranges mitochondria and has been
221 implicated in a state of suspended animation, attributed to inhibition of complex IV of the electron
222 transport chain (57, 58). The major H₂S-producing enzymes are spatially compartmentalized in the
223 adult brain, with CBS concentrated in astrocytes and CSE in neurons (29, 59). In amyotrophic
224 lateral sclerosis (ALS) caused by the G93A mutation in superoxide dismutase 1 (SOD1) and in
225 Down's Syndrome (DS), excess H₂S is neurotoxic (60-63). H₂S donors are therapeutic in several
226 AD models, however direct links to sulfhydration have not been established (43, 64-70).

227 In this study, we detected diminished expression of CSE and sulfhydration in the AD brain. The
228 3xTg-AD mouse model as well as postmortem cortex samples of AD patients display reduced
229 sulfhydration. Supplementation with the slow releasing H₂S donor, NaGYY rescues the diminished
230 sulfhydration levels in the brains of 3xTg-AD mouse model and alleviates motor and cognitive
231 deficits. Our findings concur with reports of diminished H₂S levels in serum of AD patients and
232 confirm the neuroprotective role of H₂S donors in rodent models of AD (42, 43, 64, 65, 69, 71, 72).
233 Treatment with H₂S donors ameliorated several deficits including those in learning and memory.

234 How might sulfhydration be neuroprotective? We propose that H₂S sulfhydrates GSK3 β , thereby
235 inhibiting phosphorylation of Tau and preventing neurotoxicity (Fig. 4H). As H₂S participates in
236 multiple signaling cascades, additional neuroprotective pathways may be involved (37). For
237 example, the Nuclear factor erythroid 2-related factor 2 (Nrf2) signaling pathway, which regulates
238 response to oxidative stress response, may be enhanced by H₂S. Under basal conditions, Nrf2 is
239 sequestered in the cytosol of cells by the kelch-like ECH-associated protein (Keap1), which targets

240 it for proteasomal degradation (73). Keap1 has reactive cysteine residues, which, when
241 sulfhydrated, causes its dissociation from Nrf2, which then translocates to the nucleus to transcribe
242 genes involved in stress responses (42, 74). Similarly, H₂S modulates transcriptional regulatory
243 networks which are disrupted in neurodegeneration (38, 75). Stimulating the reverse
244 transsulfuration pathway may be beneficial in AD. This pathway also leads to the production of
245 glutathione, the cellular antioxidant, which regulates redox homeostasis and neurotransmission
246 (76, 77). As the reverse transsulfuration pathway is a central hub in several neuroprotective
247 signaling networks, its stimulation may afford therapeutic benefits by restoring redox balance and
248 H₂S metabolism (28, 41). This pathway is disrupted in several neurodegenerative diseases
249 exhibiting impaired redox homeostasis. Thus in PD and HD, stimulating the production of cysteine
250 and H₂S via CSE is neuroprotective (24, 25, 38, 56). Aging is associated with diminished
251 transsulfuration, and sulfhydration as well as elevated oxidative stress. We have shown previously
252 that decreased sulfhydration and increased oxidation of cysteine residues on proteins occur across
253 evolutionary boundaries during aging (39). Additionally, aging is the greatest risk factor for
254 developing neurodegenerative diseases including AD (78). Accordingly, targeting the reverse
255 transsulfuration pathway may afford therapeutic benefits for aging and neurodegenerative diseases
256 involving suboptimal H₂S signaling.

257

258

259 **Materials and Methods**

260

261 **Cell cultures and reagents**

262

263 HEK293 cells were from American Tissue Culture Type Collection (ATCC). All chemicals were from
264 Sigma unless mentioned otherwise. In this study we used a sodium salt of derivative of the slow
265 release H₂S donor, GYY4137 (NaGYY). Use of this compound was necessary, as commercial
266 preparations of GYY4137 is a morpholine salt and complexed with unstated quantities of the
267 carcinogenic solvent methylene chloride. Morpholine and dichloromethane (methylene chloride)
268 are highly toxic and are not biologically inert with the latter well documented to be metabolized to
269 carbon monoxide. Since sodium salts are pharmaceutically acceptable and non-toxic, we therefore
270 synthesized NaGYY in-house as described previously by us to avoid these contaminants and
271 impurities (51, 52). Lipofectamine 2000 (Invitrogen) was used for all transfection studies. The
272 pRK5-eGFP-Tau (46904), pRK5-eGFP-Tau P301L (4690), pcDNA3-HA-GSK3 β (14753), and
273 pcDNA3-HA-GSK3 β S9A (14754) constructs were obtained from Addgene.

274

275 **Immunoprecipitation assays and Western blot analysis**

276 HEK293 cells were transfected with indicated plasmids 24 h prior to lysis of the cells. Cells were
277 lysed in buffer (IP buffer), containing 50 mM Tris-HCl (pH 8.0), 150 mM NaCl, 1% Triton X-100, 10

278 % glycerol protease inhibitors (cOmplete™, EDTA-free Protease Inhibitor Cocktail from Sigma) and
279 phosphatase inhibitors (PhosSTOP™ phosphatase inhibitor, Sigma) and lysates were cleared by
280 centrifugation at 16,000 g for 10 min followed by recovery of the supernatant. Protein was quantified
281 by Bradford assay and samples were normalized for protein content. Inputs were reserved and 500
282 µg of protein was incubated with GST beads overnight at 4 °C with rotation. Beads were washed
283 four times in IP buffer, followed by elution into 1X LDS buffer (Stock 4X containing 40% glycerol,
284 4% lithium dodecyl sulfate (LDS), 0.8 M triethanolamine-Cl pH 7.6, 4% Ficoll®-400, 0.025% phenol
285 red, 0.025% Coomassie G250, 2 mM EDTA disodium from Thermo Fisher Scientific, USA) with 1
286 mM DTT at 95 °C for 5 min. Samples and inputs were loaded on a mini NuPAGE 4-12% Bis-Tris
287 gel (Thermo Fisher, Scientific USA) and electrophoresed in 1X NuPAGE MES (2-(N-morpholino)
288 ethanesulfonic acid) SDS running buffer (Thermo Fisher Scientific, USA) and immunoblotted with
289 the indicated antibodies. Antibodies used include anti-CSE, generated in-house (36) (1: 4000), anti-
290 FLAG (1: 3000, Sigma), anti-GST-HRP (1:10,000, Sigma), anti-Tau (1: 1000, Santa Cruz
291 Biotechnology), anti-GFP (1:1000, Cell Signaling Technology), anti-p396Tau (1:1000, Santa Cruz
292 Biotechnology), anti-GSK3β (1: 1000, Santa Cruz Biotechnology), anti-β-actin HRP (1:10,000,
293 Santa Cruz Biotechnology). For the *in vitro* immunoprecipitation assays, either anti-Tau antibody
294 or normal mouse IgG control was incubated with Protein A/G agarose overnight at 4 °C with
295 rotation. Antibody-agarose mixture was incubated with purified wild type Tau for 6 h at 4 °C with
296 rotation, washed three times in IP buffer, and incubated with CSE overnight at 4 °C with rotation.
297 Beads were washed four times in IP buffer followed by elution into LDS buffer with 1 mM DTT at
298 95 °C for 5 min. Samples and inputs were analyzed by western blotting as described above.
299 Additional details of reagents and methods are available in *SI Appendix*.

300

301 **Acknowledgments**

302

303 This work was supported by US Public Health Service Grant DA044123 (to S.H.S) and the
304 American Heart Association (AHA)-Allen Initiative in Brain Health and Cognitive Impairment (to
305 S.H.S and associates), Medical Research Council, UK (MR/S002626/1 to MW), the Brian Ridge
306 Scholarship (RT), the European Research Council (ERC) under the European Union's Horizon
307 2020 research and innovation programme (864921 to MRF). We are grateful to Olga Pletnikova,
308 Brain Resource Center (BRC) at Johns Hopkins University for providing post-mortem AD brain
309 samples. The Johns Hopkins University Mass Spectrometry Core is acknowledged for analysis of
310 protein sulfhydrylation. We especially thank the reviewers for their valuable comments and
311 suggestions, which have greatly strengthened the study.

312

313 **Author disclosures**

314 MW, RT and the University of Exeter have patents (awarded/pending) on hydrogen sulfide delivery
315 molecules and their therapeutic use.

316

317

318 **Figure Legends**

319

320 **Fig. 1.** Cystathionine γ -lyase expression is decreased in Alzheimer's disease. (A) The reverse
321 transsulfuration pathway in mammals. Homocysteine, generated from dietary methionine, is
322 condensed with serine to generate cystathionine by cystathionine β -synthase (CBS). Cystathionine
323 is acted on by cystathionine γ -lyase (CSE) to produce cysteine. Cysteine can either be utilized to
324 synthesize glutathione and other sulfur containing molecules or used as a substrate to generate
325 hydrogen sulfide (H₂S). Both homocysteine and cysteine may be utilized to produce H₂S. While
326 CSE may generate H₂S from either cysteine or homocysteine, CBS produces H₂S using a
327 combination of cysteine and homocysteine. 3-mercaptopyruvate sulfur transferase (3-MST), in
328 conjunction with cysteine amino transferase (CAT), a third enzyme, also produces H₂S from
329 cysteine. (B) CSE is depleted in the cortex of 24-mo 3xTg-AD mice. $n=3$, SEM, $*P < 0.05$. (C) CSE
330 is depleted in the hippocampus of 3xTg-AD mice. $n=3$, SEM, $*P < 0.05$. (D) CSE is diminished in
331 the cortex of AD patients (Braak stage 6). $n=3$, SEM, $*P < 0.05$. (E) The dimedone switch assay.
332 Proteins were reacted with 4-chloro-7-nitrobenzofurazan (NBF-Cl), to label persulfides, thiols,
333 sulfenic acids, and amino groups. Reaction with amino groups specifically results in a characteristic
334 green fluorescence. Next, the NBF tag is switched by a dimedone-based probe, which emits red
335 fluorescence (the Cy5 tag is shown as a red circle), selectively labeling persulfides. The mixture is
336 then run on SDS gels and signals detected by fluorescence scanning. (F) Gel scan showing
337 reduced sulphydration in postmortem human AD brain samples and quantitation. $n=4$, SEM $*P <$
338 0.05.

339

340

341 **Fig. 2.** Cystathionine γ -lyase (CSE) binds the microtubule binding protein Tau. (A) Schematic
342 representation of full-length Tau, which is composed of 441 amino acids. Tau harbors the N
343 terminal domains, N1 and N2, a proline-rich region (PRR) and four repeat domains R1 through R4
344 which bind microtubules. Two cysteine residues Cys291 and Cys322 are present in R2 and R3
345 respectively. (B) Interaction of Tau with CSE and CBS. HEK293 cells were transfected with
346 constructs encoding Flag tagged wild type Tau (Flag-Tau) and either GST tagged CSE or CBS or
347 GST vector and GST pulldown assay conducted. GST-CSE and GST-CBS interact with Flag-Tau.
348 (C) CSE binds Tau directly. *In vitro* coimmunoprecipitation assay using purified CSE and Tau.
349 Normal IgG control was used as an isotype control for the anti-Tau antibody used in the
350 immunoprecipitation. (D) CSE and CBS do not bind to mutant Tau P301L as revealed by co-
351 immunoprecipitation assays in HEK293 cells overexpressing GST-CSE or GST-CBS and either

352 wild type Tau (WT) or mutant Tau P301L. Arrow with “s” indicates specific GFP-Tau band, arrow
353 with “ns” indicates non-specific band. (E) Wild type Tau stimulates activity of CSE *in vitro* (using
354 purified proteins) as measured by H₂S production by the methylene blue assay. *n*=3, SEM, **P* <
355 0.05. (F) Kinetics of H₂S production from human recombinant CSE without (black squares) or with
356 Tau (red dots). CSE/Tau protein molar ratio is ½. Wild type Tau stimulates activity of CSE as
357 assayed by a spectrophotometric assay utilizing 0.22 μM purified CSE and 0.44 μM in 100 mM
358 HEPES buffer (pH 7.4) containing 0.4 mM lead acetate at 37 °C for 3 min and absorbance
359 measured at 390 nm, reflecting the formation lead sulfide formed by reaction of H₂S with lead
360 acetate. (G) Wild type Tau stimulates activity of CSE in HEK 293 cells in an *in vitro* reaction
361 containing 10 mM L-cysteine and 250 μM pyridoxal 5-phosphate (PLP) as measured by H₂S
362 production by the methylene blue assay. *n*=3, SEM, ***P* < 0.01. (H) WT Tau increases the activity
363 of CSE in a time dependent manner. *n*=3, SEM, ****P* < 0.001. (I) Tau is sulfhydrated by H₂S. Flag-
364 Tau was transfected into HEK293 and treated with 100 μM NaSH and sulfhydration analyzed by
365 the modified biotin switch assay.

366
367 **Fig. 3.** CSE and H₂S inhibit phosphorylation of Tau by GSK3β. (A) Phosphorylation assays with
368 purified Tau, GSK3β and CSE *in vitro*, in the presence or absence of L-cysteine (L-cys) and
369 pyridoxal 5'-phosphate (PLP) or treated with 100 μM NaSH. Phosphorylation of Tau was assessed
370 by western blotting using antibodies against phosphorylated Tau (pTau 396). Tau phosphorylation
371 was significantly diminished when CSE, L-cysteine and PLP were added. Addition of NaSH alone,
372 in the absence of CSE also prevented Tau phosphorylation. (B) Cysteine residues do not play a
373 role in phosphorylation of Tau by GSK3β. Purified Tau or Tau C291S/C322S and GSK3β were
374 incubated in the presence or absence of L-cysteine and PLP and analyzed for phosphorylation of
375 Tau at Ser396. Western blot analysis revealed that mutation of cysteine residues Cys291 and
376 Cys322 does not affect phosphorylation of Tau at Ser396. *n*=3, SEM, **P* < 0.05, ****P* < 0.001. (C)
377 H₂S inhibits phosphorylation of P301L Tau by GSK3β. HEK293 cells were transfected with Tau
378 P301L or Tau P301L C291S/C322S and GSK3β S9A and treated with 100 μM NaSH for 24 h and
379 analyzed for phosphorylation of Tau at Ser396 by western blotting. While GSK3β phosphorylated
380 Tau, NaSH prevented this phosphorylation. (D) Ribbon Model of GSK3β (PDB:1j1b;
381 DOI: 10.1107/S090744490302938X). Intercept: (E) Thiolate side chain of Cys218 (ball and stick
382 model), that we found to be sulfhydrated, is already in a close proximity to Asp181 in the active site
383 of GSK3β, so the presence of an additional sulfur atom will inevitably alter the conformation of the
384 active site, which would inhibit its kinase activity. Oxygen atoms are shown in red, sulfur in yellow
385 and nitrogen in blue. Dots around the atoms represent expected water surface accessibility. (F)
386 Schematic representation of the antibody array-like approach to study sulfhydration status of
387 GSK3β in AD brains. Anti-GSK3β antibody was immobilized on a 96 well plate with NHS-activated

388 surface. Brain cortical lysates from normal and AD post-mortem tissues were added to the wells to
389 allow recognition of GSK3 β from lysates by the antibody. The bound protein was labeled with NBF
390 (green) for a total load and with Cy5 (red) for sulfhydrylation and the ratio of the two signals measured
391 to yield sulfhydrylation levels. As a negative control 488-labelled albumin (instead of antibody) was
392 used to block the available surface and then incubated with control lysates. (G) Read-out from a
393 representative experiment showing decreased sulfhydrylation (red) in cortex of AD patients, while
394 the negative control shows no signals. The plate was recorded on Typhoon FL9500 at 488 nm
395 (NBF fluorescence signal, green, which represents total load) and 635 nm (Cy5 signal (red), which
396 represents sulfhydrylation). (H) Quantitation of H. $n=4$, SEM, *** $P < 0.001$.

397 **Fig. 4.** The H₂S donor, NaGYY ameliorates AD symptoms. (A) Overall sulfhydrylation is decreased
398 in the hippocampus of 3xTg-AD mice, which is rescued by NaGYY treatment in 3xTg-AD mice as
399 revealed by the dimedone switch method. $n=3$, SEM, *** $P < 0.001$. (B) Sulfhydrylation of Tau is
400 decreased in the hippocampus of 3xTg-AD mice as revealed by immunoprecipitation assays in
401 combination with the dimedone switch assay. Treatment with NaGYY rescues sulfhydrylation of Tau.
402 (C) Treatment regimen for 3xTg-AD mice with the H₂S donor, NaGYY. Mice were treated at 6-mo
403 with 100 mg/kg NaGYY by intraperitoneal injection daily for 12 wk and behavioral analyses
404 conducted at 9-mo. The open field test revealed significant deficits in locomotor activity in the male
405 3xTg-AD mice, which were rescued by NaGYY. $n=6-10$, SEM, ** $P < 0.01$ and * $P < 0.05$. (D-G)
406 NaGYY partially rescues memory deficits in the 3xTg-AD mice. These mice do not exhibit
407 significant differences in primary error and total error in the Barnes Maze test (D,E). NaGYY
408 treatment partially rescues primary and total latency (F,G). $n=6-10$, SEM, * $P < 0.05$ for comparison
409 between primary latency of 3xTg-AD Saline and 3xTg-AD NaGYY by one-way ANOVA followed by
410 a post-hoc Tukey test. (H) Model depicting a possible mode of neuroprotection afforded by H₂S.
411 GSK3 β (yellow-ochre) binds Tau (purple) and phosphorylates it (depicted as "P"), which leads to
412 the formation of neurofibrillary tangles (NFTs) and AD pathology in the 3xTgAD mice. H₂S produced
413 by CSE (green) sulfhydrates GSK3 β ("SH" in red text) and inhibits phosphorylation of Tau. Tau
414 binds to CSE and enhances its activity (arrow with a "+" sign), forming part of a virtuous cycle that
415 decreases Tau phosphorylation and confers neuroprotection.

416

417

418

419 References

- 420 1. C. A. Lane, J. Hardy, J. M. Schott, Alzheimer's disease. *Eur J Neurol* **25**, 59-70 (2018).
- 421 2. C. L. Masters *et al.*, Alzheimer's disease. *Nat Rev Dis Primers* **1**, 15056 (2015).
- 422 3. J. M. Long, D. M. Holtzman, Alzheimer Disease: An Update on Pathobiology and
423 Treatment Strategies. *Cell* **179**, 312-339 (2019).

- 424 4. J. L. Cummings, T. Morstorf, K. Zhong, Alzheimer's disease drug-development pipeline:
425 few candidates, frequent failures. *Alzheimers Res Ther* **6**, 37 (2014).
- 426 5. C. M. Karch, A. M. Goate, Alzheimer's disease risk genes and mechanisms of disease
427 pathogenesis. *Biol Psychiatry* **77**, 43-51 (2015).
- 428 6. C. Ballatore, V. M. Lee, J. Q. Trojanowski, Tau-mediated neurodegeneration in
429 Alzheimer's disease and related disorders. *Nat Rev Neurosci* **8**, 663-672 (2007).
- 430 7. V. M. Lee, M. Goedert, J. Q. Trojanowski, Neurodegenerative tauopathies. *Annu Rev*
431 *Neurosci* **24**, 1121-1159 (2001).
- 432 8. T. Arendt, J. T. Stieler, M. Holzer, Tau and tauopathies. *Brain Res Bull* **126**, 238-292
433 (2016).
- 434 9. M. D. Weingarten, A. H. Lockwood, S. Y. Hwo, M. W. Kirschner, A protein factor essential
435 for microtubule assembly. *Proc Natl Acad Sci U S A* **72**, 1858-1862 (1975).
- 436 10. J. Avila, J. J. Lucas, M. Perez, F. Hernandez, Role of tau protein in both physiological
437 and pathological conditions. *Physiol Rev* **84**, 361-384 (2004).
- 438 11. T. Arakhamia *et al.*, Posttranslational Modifications Mediate the Structural Diversity of
439 Tauopathy Strains. *Cell* **180**, 633-644 e612 (2020).
- 440 12. Y. Wang, E. Mandelkow, Tau in physiology and pathology. *Nat Rev Neurosci* **17**, 5-21
441 (2016).
- 442 13. L. Martin, X. Latypova, F. Terro, Post-translational modifications of tau protein:
443 implications for Alzheimer's disease. *Neurochem Int* **58**, 458-471 (2011).
- 444 14. H. Braak, E. Braak, Staging of Alzheimer's disease-related neurofibrillary changes.
445 *Neurobiol Aging* **16**, 271-278; discussion 278-284 (1995).
- 446 15. T. Gomez-Isla *et al.*, Neuronal loss correlates with but exceeds neurofibrillary tangles in
447 Alzheimer's disease. *Ann Neurol* **41**, 17-24 (1997).
- 448 16. M. Medina, F. Hernandez, J. Avila, New Features about Tau Function and Dysfunction.
449 *Biomolecules* **6** (2016).
- 450 17. M. Jouanne, S. Rault, A. S. Voisin-Chiret, Tau protein aggregation in Alzheimer's
451 disease: An attractive target for the development of novel therapeutic agents. *Eur J Med*
452 *Chem* **139**, 153-167 (2017).
- 453 18. G. Lindwall, R. D. Cole, Phosphorylation affects the ability of tau protein to promote
454 microtubule assembly. *J Biol Chem* **259**, 5301-5305 (1984).
- 455 19. I. Grundke-Iqbal *et al.*, Abnormal phosphorylation of the microtubule-associated protein
456 tau (tau) in Alzheimer cytoskeletal pathology. *Proc Natl Acad Sci U S A* **83**, 4913-4917
457 (1986).
- 458 20. B. R. Hoover *et al.*, Tau mislocalization to dendritic spines mediates synaptic dysfunction
459 independently of neurodegeneration. *Neuron* **68**, 1067-1081 (2010).
- 460 21. J. I. Sbdio, S. H. Snyder, B. D. Paul, Redox Mechanisms in Neurodegeneration: From
461 Disease Outcomes to Therapeutic Opportunities. *Antioxid Redox Signal* **30**, 1450-1499
462 (2019).
- 463 22. V. Vitvitsky, M. Thomas, A. Ghorpade, H. E. Gendelman, R. Banerjee, A functional
464 transsulfuration pathway in the brain links to glutathione homeostasis. *J Biol Chem* **281**,
465 35785-35793 (2006).
- 466 23. L. Diwakar, V. Ravindranath, Inhibition of cystathionine-gamma-lyase leads to loss of
467 glutathione and aggravation of mitochondrial dysfunction mediated by excitatory amino
468 acid in the CNS. *Neurochem Int* **50**, 418-426 (2007).
- 469 24. B. D. Paul *et al.*, Cystathionine gamma-lyase deficiency mediates neurodegeneration in
470 Huntington's disease. *Nature* **509**, 96-100 (2014).
- 471 25. M. S. Vandiver *et al.*, Sulfhydration mediates neuroprotective actions of parkin. *Nat*
472 *Commun* **4**, 1626 (2013).
- 473 26. J. B. Kohl, A. T. Mellis, G. Schwarz, Homeostatic impact of sulfite and hydrogen sulfide
474 on cysteine catabolism. *Br J Pharmacol* **176**, 554-570 (2019).
- 475 27. N. Sen *et al.*, Hydrogen sulfide-linked sulfhydration of NF-kappaB mediates its
476 antiapoptotic actions. *Mol Cell* **45**, 13-24 (2012).

- 477 28. J. I. Sbodio, S. H. Snyder, B. D. Paul, Regulators of the transsulfuration pathway. *Br J Pharmacol* **176**, 583-593 (2019).
- 478
- 479 29. T. Morikawa *et al.*, Hypoxic regulation of the cerebral microcirculation is mediated by a carbon monoxide-sensitive hydrogen sulfide pathway. *Proc Natl Acad Sci U S A* **109**, 1293-1298 (2012).
- 480
- 481
- 482 30. B. D. Paul, S. H. Snyder, H₂S: A Novel Gasotransmitter that Signals by Sulfhydration. *Trends Biochem Sci* **40**, 687-700 (2015).
- 483
- 484 31. B. D. Paul, S. H. Snyder, Protein sulfhydration. *Methods Enzymol* **555**, 79-90 (2015).
- 485 32. B. D. Paul, S. H. Snyder, H(2)S signalling through protein sulfhydration and beyond. *Nat Rev Mol Cell Biol* **13**, 499-507 (2012).
- 486
- 487 33. M. R. Filipovic, J. Zivanovic, B. Alvarez, R. Banerjee, Chemical Biology of H₂S Signaling through Persulfidation. *Chem Rev* **118**, 1253-1337 (2018).
- 488
- 489 34. R. Wang, Physiological implications of hydrogen sulfide: a whiff exploration that blossomed. *Physiol Rev* **92**, 791-896 (2012).
- 490
- 491 35. R. Wang, Hydrogen sulfide: a new EDRF. *Kidney Int* **76**, 700-704 (2009).
- 492 36. G. Yang *et al.*, H₂S as a physiologic vasorelaxant: hypertension in mice with deletion of cystathionine gamma-lyase. *Science* **322**, 587-590 (2008).
- 493
- 494 37. B. D. Paul, S. H. Snyder, Gasotransmitter hydrogen sulfide signaling in neuronal health and disease. *Biochem Pharmacol* **149**, 101-109 (2018).
- 495
- 496 38. J. I. Sbodio, S. H. Snyder, B. D. Paul, Transcriptional control of amino acid homeostasis is disrupted in Huntington's disease. *Proc Natl Acad Sci U S A* **113**, 8843-8848 (2016).
- 497
- 498 39. J. Zivanovic *et al.*, Selective Persulfide Detection Reveals Evolutionarily Conserved Antiaging Effects of S-Sulfhydration. *Cell Metab* **30**, 1152-1170 e1113 (2019).
- 499
- 500 40. W. Droge, Oxidative stress and ageing: is ageing a cysteine deficiency syndrome? *Philos Trans R Soc Lond B Biol Sci* **360**, 2355-2372 (2005).
- 501
- 502 41. B. D. Paul, J. I. Sbodio, S. H. Snyder, Cysteine Metabolism in Neuronal Redox Homeostasis. *Trends Pharmacol Sci* **39**, 513-524 (2018).
- 503
- 504 42. Y. Liu *et al.*, Hydrogen sulfide ameliorates learning memory impairment in APP/PS1 transgenic mice: A novel mechanism mediated by the activation of Nrf2. *Pharmacol Biochem Behav* **150-151**, 207-216 (2016).
- 505
- 506
- 507 43. A. Xuan *et al.*, Hydrogen sulfide attenuates spatial memory impairment and hippocampal neuroinflammation in beta-amyloid rat model of Alzheimer's disease. *J Neuroinflammation* **9**, 202 (2012).
- 508
- 509
- 510 44. S. Oddo *et al.*, Triple-transgenic model of Alzheimer's disease with plaques and tangles: intracellular Abeta and synaptic dysfunction. *Neuron* **39**, 409-421 (2003).
- 511
- 512 45. H. Takuma, S. Arawaka, H. Mori, Isoforms changes of tau protein during development in various species. *Brain Res Dev Brain Res* **142**, 121-127 (2003).
- 513
- 514 46. P. McMillan *et al.*, Tau isoform regulation is region- and cell-specific in mouse brain. *J Comp Neurol* **511**, 788-803 (2008).
- 515
- 516 47. D. P. Hanger, B. H. Anderton, W. Noble, Tau phosphorylation: the therapeutic challenge for neurodegenerative disease. *Trends Mol Med* **15**, 112-119 (2009).
- 517
- 518 48. B. H. Anderton *et al.*, Sites of phosphorylation in tau and factors affecting their regulation. *Biochem Soc Symp* 10.1042/bss0670073, 73-80 (2001).
- 519
- 520 49. Y. Zhao, H. Wang, M. Xian, Cysteine-activated hydrogen sulfide (H₂S) donors. *J Am Chem Soc* **133**, 15-17 (2011).
- 521
- 522 50. L. Li *et al.*, Characterization of a novel, water-soluble hydrogen sulfide-releasing molecule (GYY4137): new insights into the biology of hydrogen sulfide. *Circulation* **117**, 2351-2360 (2008).
- 523
- 524
- 525 51. M. Whiteman *et al.*, Phosphinodithioate and Phosphoramidodithioate Hydrogen Sulfide Donors. *Handb Exp Pharmacol* **230**, 337-363 (2015).
- 526
- 527 52. B. E. Alexander *et al.*, Investigating the generation of hydrogen sulfide from the phosphoramidodithioate slow-release donor GYY4137. *MedChemComm* **6**, 1649-1655 (2015).
- 528
- 529

- 530 53. E. Latorre, R. Torregrossa, M. E. Wood, M. Whiteman, L. W. Harries, Mitochondria-
531 targeted hydrogen sulfide attenuates endothelial senescence by selective induction of
532 splicing factors HNRNPD and SRSF2. *Aging (Albany NY)* **10**, 1666-1681 (2018).
- 533 54. J. M. Wagner *et al.*, Analysis of Motor Function in the Tg4-42 Mouse Model of
534 Alzheimer's Disease. *Front Behav Neurosci* **13**, 107 (2019).
- 535 55. J. Voglein *et al.*, Clinical, pathophysiological and genetic features of motor symptoms in
536 autosomal dominant Alzheimer's disease. *Brain* **142**, 1429-1440 (2019).
- 537 56. J. I. Sbdio, S. H. Snyder, B. D. Paul, Golgi stress response reprograms cysteine
538 metabolism to confer cytoprotection in Huntington's disease. *Proc Natl Acad Sci U S A*
539 **115**, 780-785 (2018).
- 540 57. E. Blackstone, M. Morrison, M. B. Roth, H₂S induces a suspended animation-like state in
541 mice. *Science* **308**, 518 (2005).
- 542 58. B. D. Paul, S. H. Snyder, K. Kashfi, Effects of hydrogen sulfide on mitochondrial function
543 and cellular bioenergetics. *Redox Biol* **38**, 101772 (2020).
- 544 59. Y. Enokido *et al.*, Cystathionine beta-synthase, a key enzyme for homocysteine
545 metabolism, is preferentially expressed in the radial glia/astrocyte lineage of developing
546 mouse CNS. *FASEB J* **19**, 1854-1856 (2005).
- 547 60. A. Ichinohe *et al.*, Cystathionine beta-synthase is enriched in the brains of Down's
548 patients. *Biochem Biophys Res Commun* **338**, 1547-1550 (2005).
- 549 61. T. Panagaki, E. B. Randi, F. Augsburger, C. Szabo, Overproduction of H₂S, generated by
550 CBS, inhibits mitochondrial Complex IV and suppresses oxidative phosphorylation in
551 Down syndrome. *Proc Natl Acad Sci U S A* **116**, 18769-18771 (2019).
- 552 62. A. Davoli *et al.*, Evidence of hydrogen sulfide involvement in amyotrophic lateral
553 sclerosis. *Ann Neurol* **77**, 697-709 (2015).
- 554 63. P. Kamoun, M. C. Belardinelli, A. Chabli, K. Lallouchi, B. Chadeaux-Vekemans,
555 Endogenous hydrogen sulfide overproduction in Down syndrome. *Am J Med Genet A*
556 **116A**, 310-311 (2003).
- 557 64. D. Giuliani *et al.*, Hydrogen sulfide slows down progression of experimental Alzheimer's
558 disease by targeting multiple pathophysiological mechanisms. *Neurobiol Learn Mem* **104**,
559 82-91 (2013).
- 560 65. E. Vandini *et al.*, Mechanisms of Hydrogen Sulfide against the Progression of Severe
561 Alzheimer's Disease in Transgenic Mice at Different Ages. *Pharmacology* **103**, 50-60
562 (2019).
- 563 66. X. L. He *et al.*, Hydrogen sulfide improves spatial memory impairment and decreases
564 production of Abeta in APP/PS1 transgenic mice. *Neurochem Int* **67**, 1-8 (2014).
- 565 67. F. L. Zhao *et al.*, AP39, a Mitochondria-Targeted Hydrogen Sulfide Donor, Supports
566 Cellular Bioenergetics and Protects against Alzheimer's Disease by Preserving
567 Mitochondrial Function in APP/PS1 Mice and Neurons. *Oxid Med Cell Longev* **2016**,
568 8360738 (2016).
- 569 68. M. M. Hu *et al.*, Sumoylation Promotes the Stability of the DNA Sensor cGAS and the
570 Adaptor STING to Regulate the Kinetics of Response to DNA Virus. *Immunity* **45**, 555-
571 569 (2016).
- 572 69. X. J. Cheng *et al.*, Tacrine-Hydrogen Sulfide Donor Hybrid Ameliorates Cognitive
573 Impairment in the Aluminum Chloride Mouse Model of Alzheimer's Disease. *ACS Chem*
574 *Neurosci* **10**, 3500-3509 (2019).
- 575 70. X. L. He *et al.*, Hydrogen sulfide down-regulates BACE1 and PS1 via activating PI3K/Akt
576 pathway in the brain of APP/PS1 transgenic mouse. *Pharmacol Rep* **68**, 975-982 (2016).
- 577 71. L. Cao *et al.*, Hydrogen sulfide inhibits ATP-induced neuroinflammation and Abeta1-42
578 synthesis by suppressing the activation of STAT3 and cathepsin S. *Brain Behav Immun*
579 **73**, 603-614 (2018).
- 580 72. R. Guzman *et al.*, Protective effect of sulfurous water in peripheral blood mononuclear
581 cells of Alzheimer's disease patients. *Life Sci* **132**, 61-67 (2015).
- 582 73. J. D. Hayes, A. T. Dinkova-Kostova, The Nrf2 regulatory network provides an interface
583 between redox and intermediary metabolism. *Trends Biochem Sci* **39**, 199-218 (2014).

- 584 74. G. Yang *et al.*, Hydrogen sulfide protects against cellular senescence via S-sulphydration
585 of Keap1 and activation of Nrf2. *Antioxid Redox Signal* **18**, 1906-1919 (2013).
- 586 75. A. Kumar, M. Vaish, R. R. Ratan, Transcriptional dysregulation in Huntington's disease: a
587 failure of adaptive transcriptional homeostasis. *Drug Discov Today* **19**, 956-962 (2014).
- 588 76. T. W. Sedlak *et al.*, The glutathione cycle shapes synaptic glutamate activity. *Proc Natl*
589 *Acad Sci U S A* **116**, 2701-2706 (2019).
- 590 77. H. J. Forman, H. Zhang, A. Rinna, Glutathione: overview of its protective roles,
591 measurement, and biosynthesis. *Mol Aspects Med* **30**, 1-12 (2009).
- 592 78. Y. Hou *et al.*, Ageing as a risk factor for neurodegenerative disease. *Nat Rev Neurol* **15**,
593 565-581 (2019).

594

595

596

597

598

599

600

601

602

603

604

605

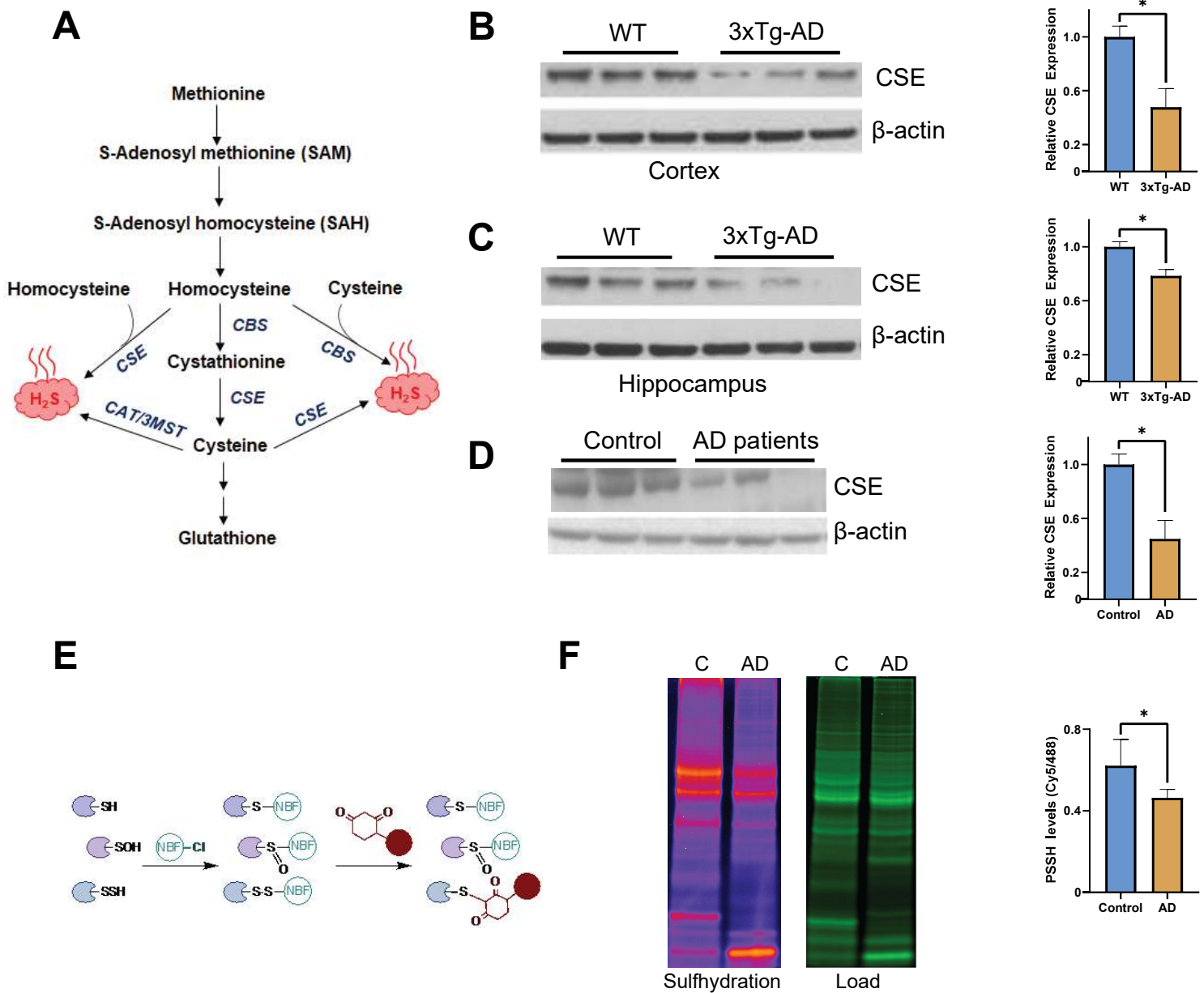


Figure 1

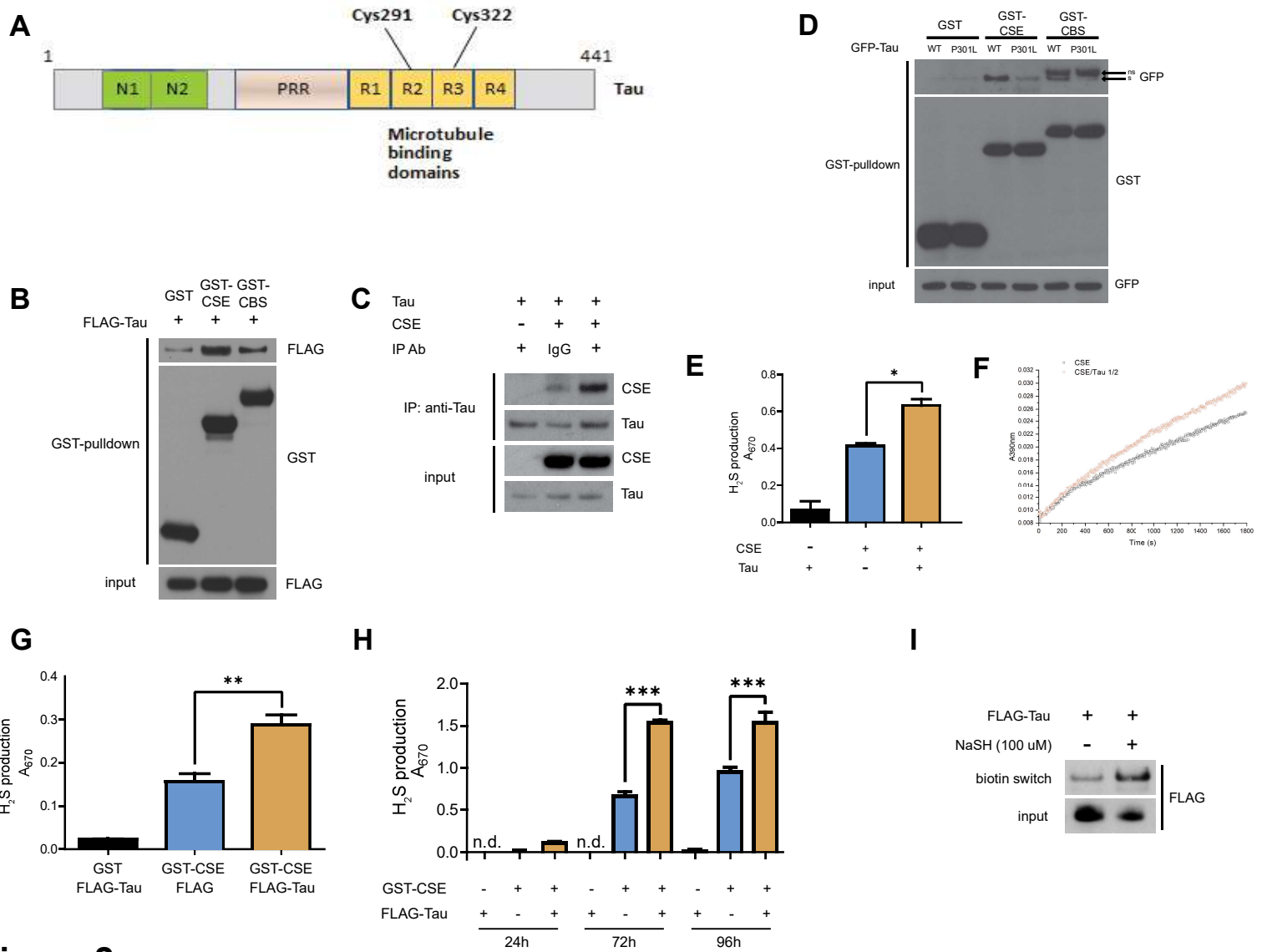


Figure 2

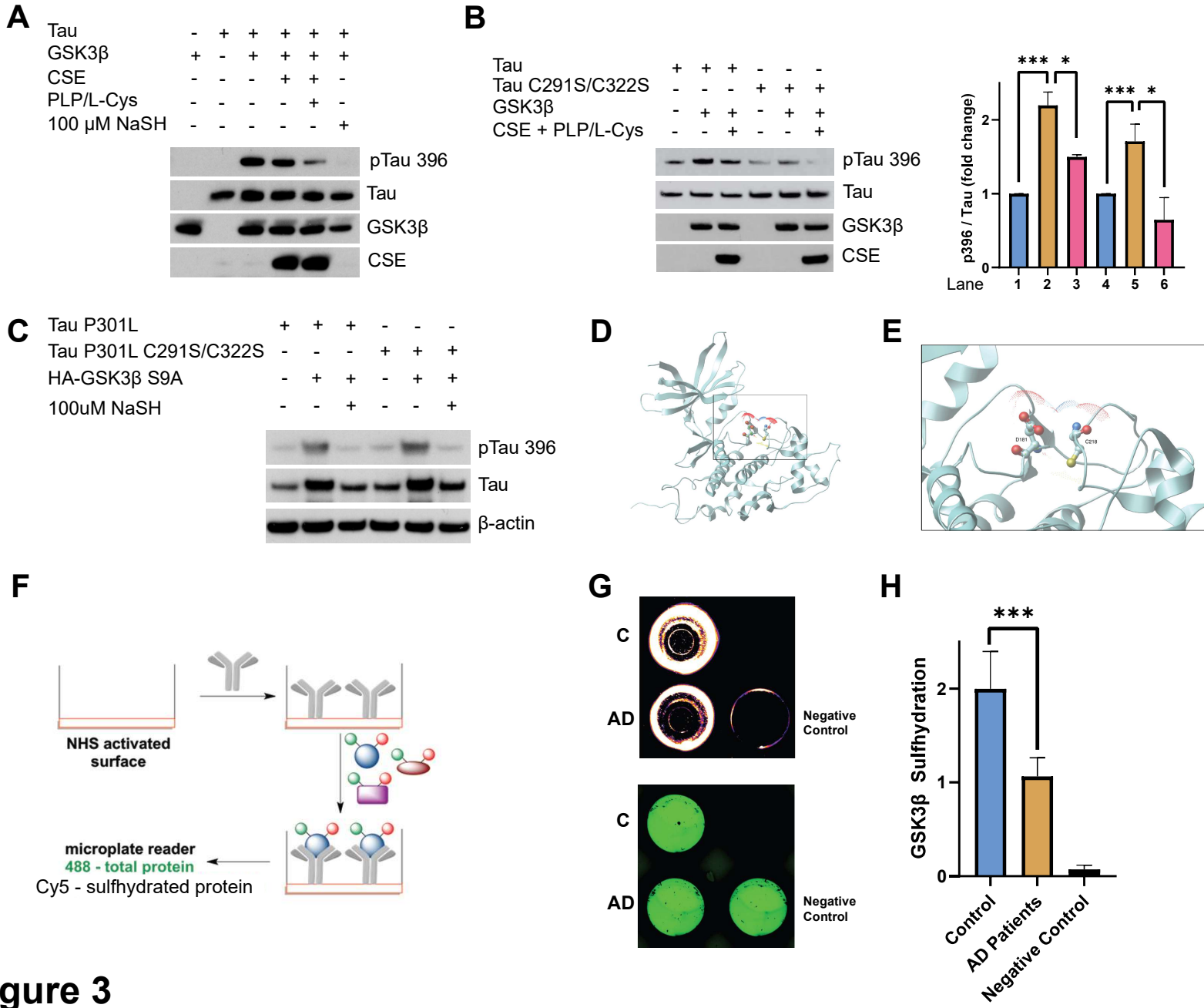


Figure 3

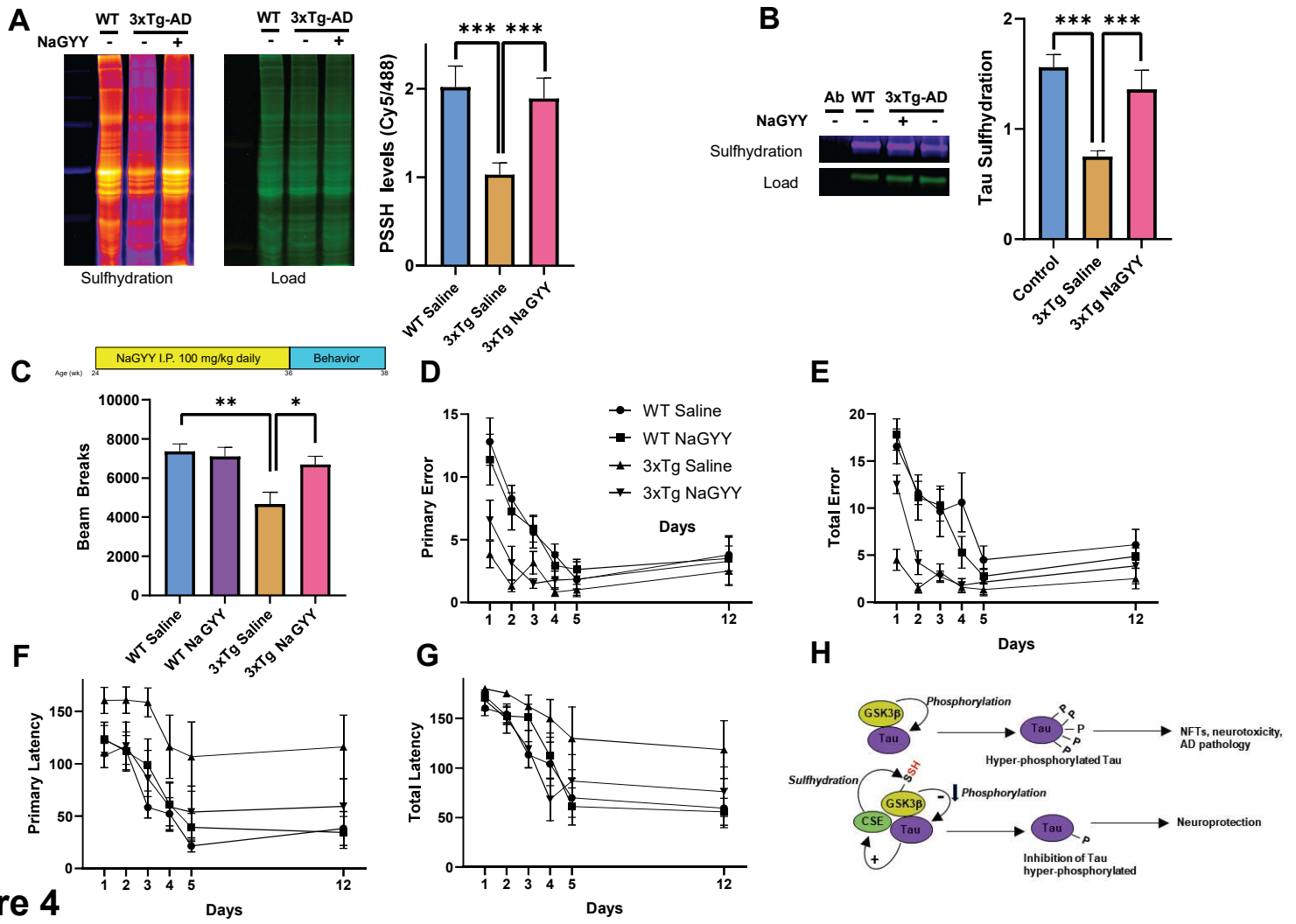


Figure 4

PNAS

www.pnas.org

Supplementary Information for

Hydrogen sulfide is neuroprotective in Alzheimer's disease by sulfhydrating GSK3 β and inhibiting Tau hyperphosphorylation.

Daniel Giovinazzo¹, Biljana Bursac⁵, Juan I Sbodio¹, Sumedha Nalluru¹, Thibaut Vignane⁵, Adele M. Snowman¹, Lauren M. Albacarys¹, Thomas W. Sedlak², Roberta Torregrossa⁴, Matthew Whiteman⁴, Milos R. Filipovic⁵, Solomon H. Snyder^{1,2,3*} and Bindu D. Paul^{1*}

*Solomon H. Snyder; *Bindu D. Paul

Email: ssnyder@jhmi.edu
bpaul8@jhmi.edu

This PDF file includes:

Supplementary Materials and Methods
Figs. S1 to S5
Legends to figures S1 to S5
References for SI reference citations

Supplementary Information Text

Materials and Methods

Use of the H₂S donor, NaGYG

In this study we have used a sodium salt of an established H₂S generating molecule, GYG4137, NaGYG (1, 2). The reasons for this were due to confounding chemicals present in commercial sources of GYG4137, sold through all major research chemical suppliers is a morpholine salt, present at a 1:1 ratio with the parent compound. However, morpholine itself is biologically active and highly toxic with a well characterized toxicity profile, and LD50 at doses commonly used for GYG4137 (e.g. 200-400 mg/kg i.p.; <http://www.inchem.org/documents/ehc/ehc/ehc179.htm>). As such its presence would confound interpretation of results generated. In addition, commercial GYG4137 contains an undisclosed amount of carcinogenic solvent (dichloromethane) present as part of the crystal lattice structure (as xCHCl₂) and it is well known to be metabolized to carbon monoxide *in vivo*. This is particularly complicated since the CO and H₂S have similar pharmacological properties and it is possible that many of the reported effects of commercially sourced GYG4137 *in vivo* may be due to CO rather than H₂S. Moreover, with undisclosed amounts of dichloromethane (at least 0.5 molecules per molecule of GYG4137 (2), the molecular mass of commercial compound is not accurate e.g. molecular weight of commercial GYG4137 is 376.6 with additional unknown quantities of dichloromethane mwt-84.9 (so an additional 22% to the final mass. For these reasons, we have used the pharmaceutically more acceptable sodium salt which is devoid of these confounding chemicals (2, 3). The decomposition (hydrolysis) pathway and H₂S generation are identical and both salts are freely water soluble which offer considerable advantages over H₂S releasing molecules which require organic solvents such as DMSO or ethanol (themselves biologically active) such as dithiolethione and thiohydroxybenzamide derivatives (1, 2).

Animals and treatment

The 3xTg-AD mouse model was obtained from Jackson laboratories (Bar Harbor, Maine). Animals were housed on a 12-h light–dark schedule and received food and water ad libitum. 6-mo old 3xTg-AD mice and their wild type controls were injected with either 100 mg/kg NaGYG or vehicle (saline) intraperitoneally for 12 wk and behavioral studies conducted at 9-mo.

Post-mortem brain samples

Post-mortem samples from normal and AD patients (Braak stage 6) were obtained from the Johns Hopkins Brain Center from J. Troncoso and O. Pletnikova.

Hydrogen sulfide production assays

HEK293 cells were transfected with indicated plasmids for the indicated time periods. For experiments with purified protein, purified recombinant CSE and Tau was used. Lysates or purified proteins were incubated for 6 h at 37 °C purged with nitrogen in 100 mM K⁺ PBS, .5% Triton X-100, 50 μM pyridoxal phosphate, 10 mM cysteine. Samples were injected with 125 μL 1% zinc acetate and 2.5 μL 10 N NaOH and incubated shaking at RT for 1 h. 500 μL of deionized water, 100 μL 20 mM N-N-dimethyl-p-phenylenediamine sulfate in 7.2M HCl, and 100 μL 30 mM FeCl₃ in 1.2M HCl were added to each sample and absorbance at 670 nm was subsequently measured. In addition, production of H₂S by CSE was measured in a spectrophotometric assay in which the reaction of H₂S with lead acetate to form lead sulfide was monitored at 390nm (4). Reaction buffer contained 1 mM of cysteine and 0.4 mM lead acetate in HEPES buffer (50 mM, pH 7.4) at 37 °C. hCSE (0.22 μM) or hCSE/hTau (0.22 μM/0.44 μM) were preincubated for 5 minutes at 37 °C (to allow the interaction and activation of the enzyme) before they were added into the buffer. H₂S production was monitored for 30 minutes by measuring the absorbance spectrum every 4 seconds. The reaction between lead acetate and L-cysteine in HEPES buffer was used as a control.

Sulfhydration/persulfidation assays

Sulfhydration assays were conducted using the modified biotin switch assay, the dimedone switch assay and by mass spectrometry as described previously (5-7). Briefly, HEK293 cells were transfected with wild type Tau for 24 h and treated with 100 μM NaSH for 24 h, as indicated. Cells were lysed in HEN buffer (250 mM HEPES–NaOH, pH 7.7, 1 mM EDTA, 0.1 mM Neocuproine) with 1% Triton X100, protease, and phosphatase inhibitors and cleared by centrifugation at 16,000 g at 4 °C for 10 min. Protein was quantified by Bradford assay and samples were normalized for protein content. Sample free thiols were blocked in methyl methanethiosulfonate (MMTS) at 50 °C for 20 min with shaking. Protein in samples was precipitated with cold acetone and washed twice with at RT with 70% acetone. Protein pellets were resuspended in HENS (HEN buffer with 1% SDS) buffer and biotin-HPDP for biotinylation of sulfhydrated cysteines. Samples were incubated for 75 min at RT with rotation. Proteins were precipitated twice with cold acetone followed by resuspension in HENS buffer. Neutralization buffer (20 mM HEPES-NaOH, pH 7.7, 100 mM NaCl, 1 mM EDTA, 0.5% Triton X-100) was added, and inputs were reserved for loading on SDS-PAGE. Neutravidin agarose beads were added to the samples and incubated at 4 °C overnight with rotation. Beads were washed with neutralization buffer with high salt (Neutralization buffer with 600 mM NaCl) seven times followed by addition of elution buffer (20 mM HEPES-NaOH, pH 7.7, 100 mM NaCl, 1 mM EDTA, 1% β-mercaptoethanol) and incubation at 95 °C for 5 min. LDS buffer with DTT was added and samples were loaded on SDS-PAGE and immunoblotted with indicated antibodies. The dimedone switch assay was conducted essentially as described earlier (6).

Mass Spectrometry for Identification of Sulfhydrated Cysteines

Purified GST-GSK3 β was incubated with 100 μ M NaSH in HEN buffer (HEPES–NaOH, pH 7.7, 250 mM EDTA, 1 mM Neocuproine 0.1 mM) for 1 h at 37 °C followed by FASP digest on a 30 kDa filter by trypsin overnight at 37 °C. Filter was washed, acidified, and peptides were eluted with 60% ACN/.1% TFA and were run immediately on high-resolution mass spectrometry for analysis. MS-MS spectra was searched using PEAKSX against the database created from MASCOT. Fragment Mass Error Tolerance was 0.012 Da and Parent Mass Error Tolerance was 6 ppm. MASCOT was set to search NP_002084.2 (glycogen synthase kinase-3 beta isoform 1 [*Homo sapiens*]). Human recombinant Tau 441 was incubated with H₂O₂ and H₂S mixture to induce protein persulfidation and labeled with dimedone switch method as described earlier (39). Untreated samples served as a control. Proteins were subjected to trypsin digestion and LC/MS/MS analysis. Obtained spectra were analyzed with PEAKSX. The search settings were: precursor Δ m tolerance = 10 ppm, fragment Δ m tolerance = 0.2 Da, missed cleavages = 2, $-10\log P > 50$, modifications of lysine: NBF (163.0012), modifications of cysteine: NBF (163.0012), dimedone (138.0681),

Purified Recombinant proteins

WT Tau and Tau C291S/C322S were purified from BL21 bacterial cells transformed with pTrcHis-Tau or pTrcHis-Tau C291S/C322S, respectively. Site-directed mutagenesis was carried out to generate the Tau mutant plasmid. Capturem His-Tagged Purification Maxiprep Columns (Takara) were used to purify the recombinant Tau proteins and visualized by SDS gel electrophoresis on 4-12% Bis-Tris polyacrylamide gels, followed by Coomassie staining using SimplyBlue SafeStain (Thermo Fisher Scientific). GST-CSE was purified by affinity chromatography using glutathione-agarose (Sigma) as per the manufacturer's recommendations.

Tau phosphorylation assays

HEK293 cells were transfected with indicated plasmids for 24 h. Cells were treated with 100 μ M NaSH for 24 h and then lysed in IP buffer with clearance of lysates by centrifugation at 16,000 g for 10 min. Protein was quantified by Bradford assay and samples were normalized for protein content. LDS buffer with DTT was added and samples incubated at 95 °C for 5 min. Samples were loaded on SDS-PAGE and immunoblotted with indicated antibodies. For the *in vitro* assays, the kinase activity assay provided with the SignalChem GSK3 β purified protein. Either 10 μ L of GSK3 β (0.02 μ g/ μ L) diluted in kinase dilution buffer III (KDBIII), containing 5 mM MOPS, pH 7.2, 2.5 mM β -glycerophosphate, 5 mM MgCl₂, 1 mM EGTA, 0.4 mM EDTA and 50 ng/ μ L BSA or 10 μ L of KDBIII, 5 μ L of 15 μ M purified Tau, and 5 μ L of dH₂O or 0.5 mM NaSH in dH₂O (stock solution). Subsequently 5 μ L of 0.25 mM ATP was added to each reaction and incubated in the shaking incubator for 15 min at 30 °C. Next, LDS (+DTT) was added to stop the reactions and incubated at 95 °C heat block for 5 min followed by Western blot analysis.

Radioactive assay for determination of GSK3 β activity: For the radioactive *in vitro* assays, the kinase activity assay using GSK3 β purified protein (SignalChem) was utilized. Either 10 μ L of GSK3 β (0.02 μ g/ μ L) diluted in kinase dilution buffer III (KDBIII), containing 5 mM MOPS, pH 7.2, 2.5 mM β -glycerophosphate, 5 mM MgCl₂, 1 mM EGTA, 0.4 mM EDTA and 50 ng/ μ L BSA or 10 μ L of KDBIII, 5 μ L of 15 μ M purified Tau, and 5 μ L of dH₂O or 0.5 mM NaSH in dH₂O (stock solution). Subsequently 5 μ L of 0.25 mM [γ -³²P] ATP (1 mCi/100 μ l) was added to each reaction and incubated in the shaking incubator for 15 min at 30 °C. Next, the reaction mixture was spotted onto individually precut strips of phosphocellulose P81 paper, which were air dried and washed with 1% phosphoric acid in double distilled water and subjected to scintillation counting to estimate the radioactivity incorporated into the peptide.

Mouse behavioral studies

Barnes maze test: 6-mo old WT and 3xTg-AD mice were treated with daily intraperitoneal injections of NaGYG (100 mg/kg) or saline (vehicle) as indicated for 12 wk until behavioral assays were performed as indicated at 9-mo. Mice were trained on the Barnes Maze platform twice a day for four days followed by testing on the fifth and twelfth days. Training and testing were carried out as follows: mice were placed in the middle of a raised platform with visual cues in the periphery and 20 holes along the edge, one of which contained an escape path for the mouse. For a maximum of three min, the number of nose pokes into correct and incorrect holes as well as the time until the mouse nose poked the correct hole and the time until the mouse entered the escape path were recorded. If a mouse entered the escape path prior to the three-min limit, the session was cut short.

Open field test. The mouse cohort used for the Barnes maze test was run on an open field chamber with IR beams recording their locomotor activity. Mice were allowed to freely roam the chamber for 45 min.

Antibody array assessment of GSK3 β sulfhydrylation. Antibody-array like detection of GSK3 β sulfhydrylation from human brain samples. The GSK3 β antibody (sc-377213, Santa Cruz) was immobilized on a 96 well plate with NHS-activated surface as described previously (6). Considering that proteins are labelled with NBF (green) for total load and with Cy5 (red) for sulfhydrylation, measuring the ratio of the two signals yields the levels of GSK3b sulfhydrylation. As a negative control 488-labelled albumin (instead of antibody) was used to block the available surface and then incubated with control lysates.

Statistical Analysis. Results are presented as means \pm SEM for at least three independent experiments. The sample sizes used were based on the magnitude of changes and consistency expected. Statistical significance was reported as appropriate. *P* values were calculated with Student's *t* test. In behavioral analyses, the experimenter conducting the test was blinded to the genotype or treatment of the animals under study. Statistical significance was calculated using one-way ANOVA/post-hoc Tukey test.

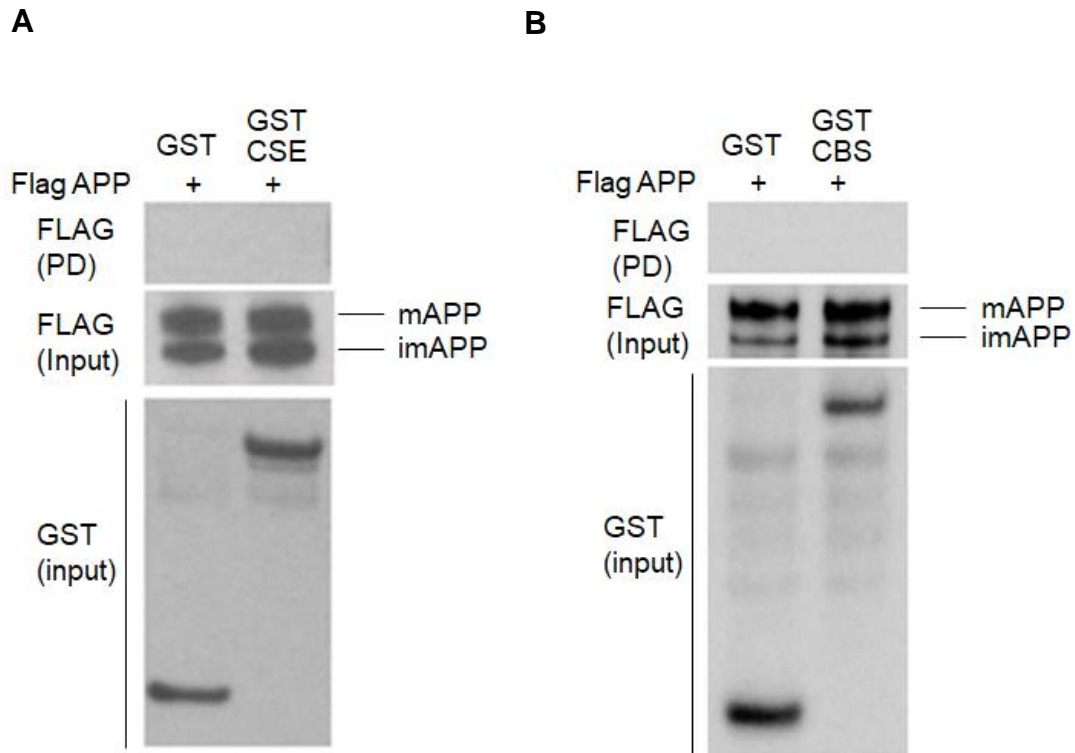


Fig. S1. Amyloid precursor protein (APP) does not interact with cystathionine γ -lyase (CSE) and cystathionine β -synthase (CBS). (A) CSE does not bind APP. HEK293 cells were transfected with FLAG APP and either GST alone or GST-CSE for 24 h and GST pulldown conducted using glutathione agarose. Western blot analysis was performed after the pull-down, APP exists in cells as two forms, the immature form (imAPP), which is *N*-glycosylated and *O*-glycosylated. CSE does not bind to APP as seen in the pull-down (PD) using anti-FLAG antibodies. (B) CBS does not bind APP. HEK293 cells were transfected and processed as described above and analyzed by Western blot analysis.

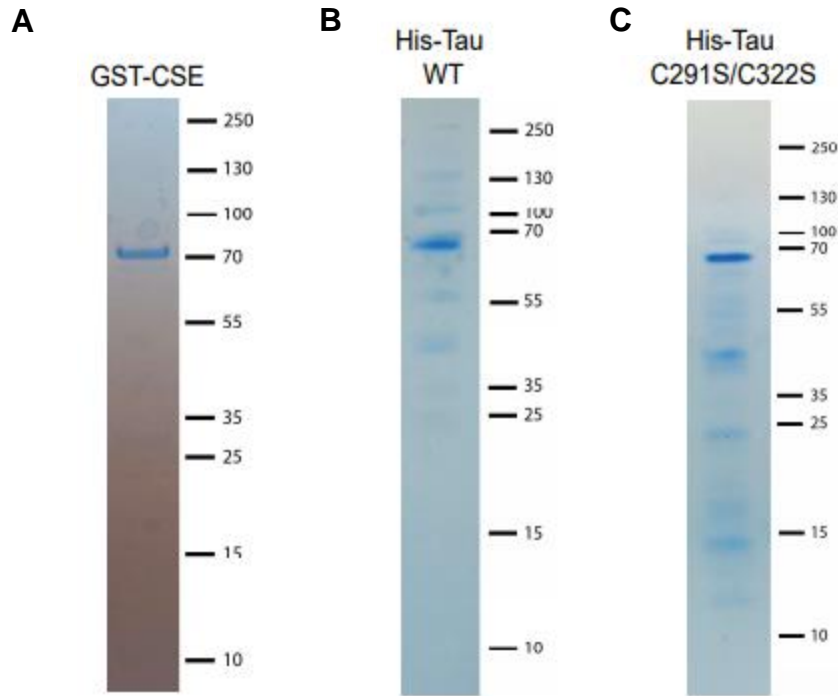


Fig. S2. Protein purification profiles of Tau, its mutants and cystathionine γ -lyase (CSE). (A) GST- tagged CSE was purified using glutathione agarose and analyzed by Coomassie staining. (B,C) His-tagged wild type Tau and the double cysteine mutant, Tau C291S/C322S was purified using CaptureEm purification systems (Takara) and purity confirmed by SDS gel electrophoresis and Coomassie staining as described earlier.

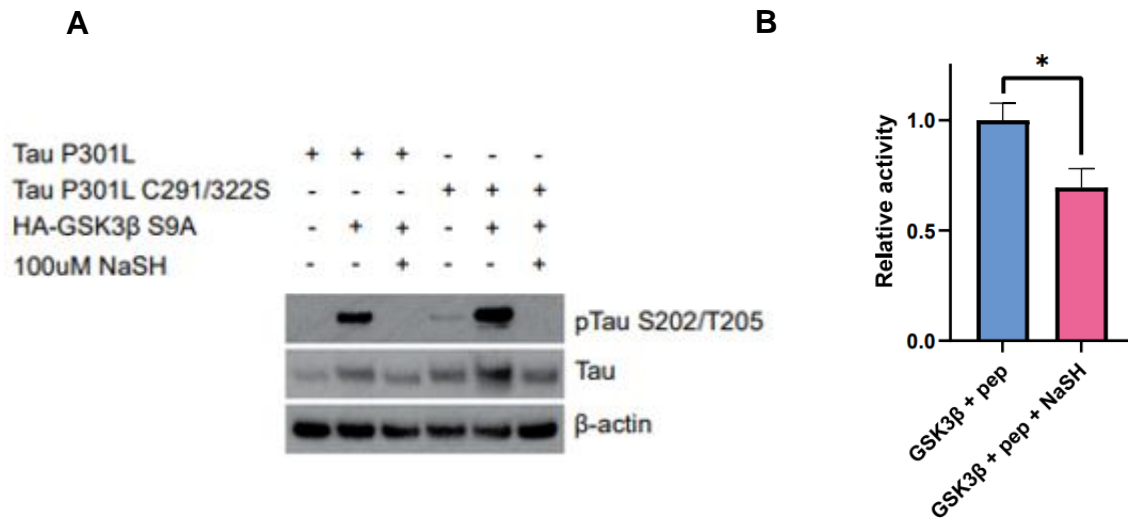


Fig. S3. Glycogen synthase kinase 3 β (GSK3 β) activity assays. (A) H₂S inhibits phosphorylation of Tau P301L by GSK3 β . HEK293 cells were transfected with Tau P301L or Tau P301LCys291/Cys322 and GSK3 β and treated with 100 μ M NaSH for 24 h and analyzed for phosphorylation of Tau at Ser202 and Thr205 by western blotting. While GSK3 β phosphorylated Tau, NaSH prevented this phosphorylation. (B) The H₂S donor, NaSH prevents phosphorylation of a peptide substrate of Tau by GSK3 β (YRRAAVPPSPSLSRHSSPHQpSEDEE, derived from glycogen synthase). Active GSK3 β , peptide substrate and [γ -³²P]-ATP were incubated at 30 °C for 15 min, followed by (n=6, SEM, **P* < 0.05).

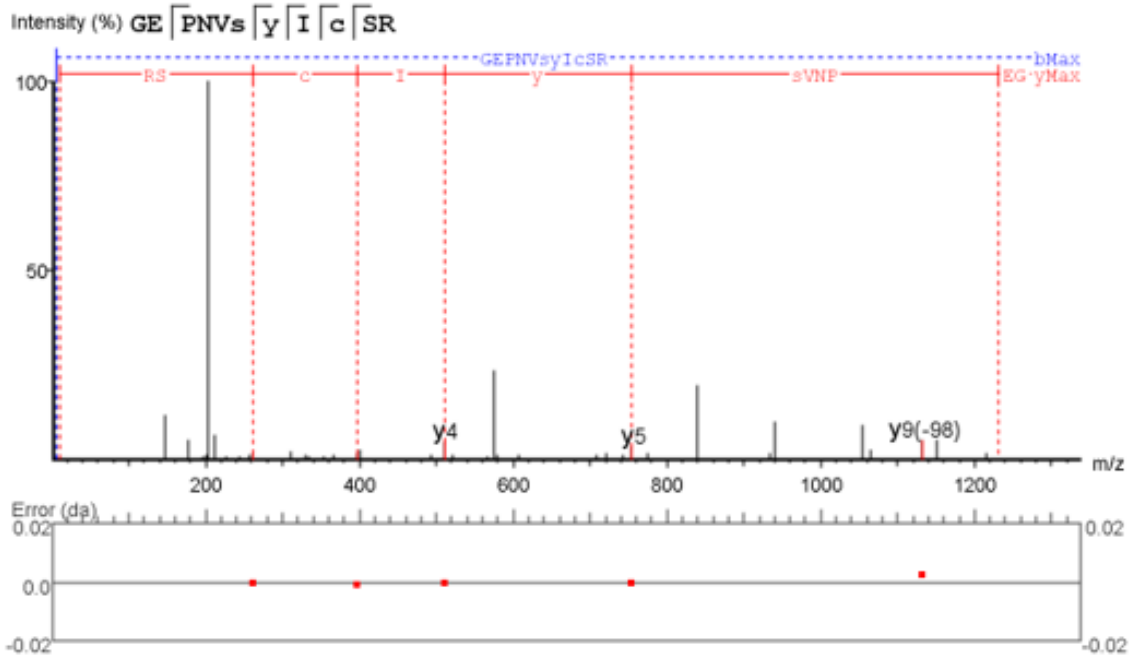


Fig. S4. LC-MS/MS spectra for identification of sulfhydration of GSK3β at Cysteine 218.

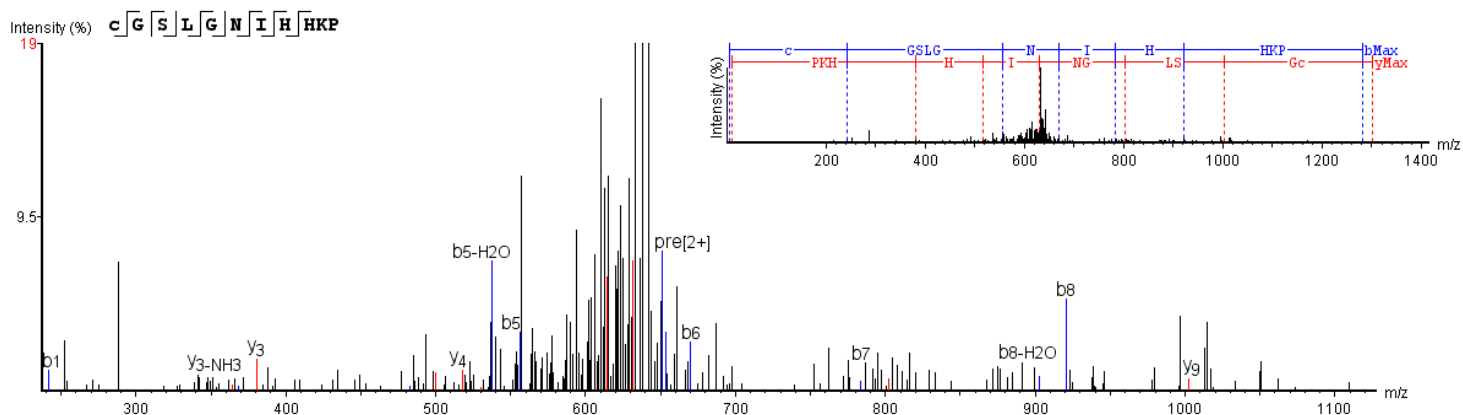


Fig. S5. MS/MS spectra of sulfhydrated C322 containing peptide of Tau labelled with dimedone, using dimedone switch method.

SI References

1. M. Whiteman *et al.*, Phosphinodithioate and Phosphoramidodithioate Hydrogen Sulfide Donors. *Handb Exp Pharmacol* **230**, 337-363 (2015).
2. B. E. Alexander *et al.*, Investigating the generation of hydrogen sulfide from the phosphonamidodithioate slow-release donor GYY4137. *MedChemComm* **6**, 1649-1655 (2015).
3. E. Latorre, R. Torregrossa, M. E. Wood, M. Whiteman, L. W. Harries, Mitochondria-targeted hydrogen sulfide attenuates endothelial senescence by selective induction of splicing factors HNRNPD and SRSF2. *Aging (Albany NY)* **10**, 1666-1681 (2018).
4. T. Chiku *et al.*, H₂S biogenesis by human cystathionine gamma-lyase leads to the novel sulfur metabolites lanthionine and homolanthionine and is responsive to the grade of hyperhomocysteinemia. *J Biol Chem* **284**, 11601-11612 (2009).

5. A. K. Mustafa *et al.*, H₂S signals through protein S-sulfhydration. *Sci Signal* **2**, ra72 (2009).
6. J. Zivanovic *et al.*, Selective Persulfide Detection Reveals Evolutionarily Conserved Antiaging Effects of S-Sulfhydration. *Cell Metab* **30**, 1152-1170 e1113 (2019).
7. M. S. Vandiver *et al.*, Sulfhydration mediates neuroprotective actions of parkin. *Nat Commun* **4**, 1626 (2013).